



Published in final edited form as:

J Thromb Haemost. 2020 August ; 18(8): 1884–1892. doi:10.1111/jth.14861.

Comprehensive N- and O-glycosylation mapping of human coagulation factor V

Cheng Ma¹, Ding Liu¹, Dong Li², Junping Zhang³, Xiao-Qian Xu⁴, He Zhu¹, Xiu-Feng Wan^{5,6,7,8,9,10}, Carol H. Miao^{11,12}, Barbara A. Konkle^{12,13}, Philip Onigman¹⁴, Weidong Xiao³, Lei Li¹

¹Department of Chemistry, Georgia State University, Atlanta, GA, USA

²Department of Clinical Laboratory, Shanghai Tongji Hospital, Tongji University School of Medicine, Shanghai, China

³Department of Microbiology and Immunology, Sol Sherry Thrombosis Research Center, Cardiovascular Research Center, Temple University, Philadelphia, PA, USA

⁴Department of Hematology, Shanghai Jiaotong University Affiliated Shanghai General Hospital, Shanghai, China

⁵Missouri University Center for Research on Influenza Systems Biology (CRISB), University of Missouri, Columbia, MO, USA

⁶Department of Molecular Microbiology and Immunology, School of Medicine, University of Missouri, Columbia, MO, USA

⁷Department of Electrical Engineering & Computer Science, College of Engineering, University of Missouri, Columbia, MO, USA

⁸Bond Life Sciences Center, University of Missouri, Columbia, MO, USA

⁹MU Informatics Institute, University of Missouri, Columbia, MO, USA

¹⁰Department of Pathobiology, College of Veterinary Medicine, University of Missouri, Columbia, MO, USA

¹¹Center for Immunity and Immunotherapies, Seattle Children's Research Institute, Seattle, WA, USA

¹²University of Washington, Seattle, WA, USA

Correspondence: Weidong Xiao, Department of Microbiology and Immunology, Sol Sherry Thrombosis Research Center, Cardiovascular Research Center, Temple University, Philadelphia, PA 19140, USA. wxiao@temple.edu, Lei Li, Department of Chemistry, Georgia State University, Atlanta, GA 30303, USA, lli22@gsu.edu.
C.M. and D.L. contributed equally to this article.

AUTHOR CONTRIBUTIONS

Cheng Ma, Ding Liu, Weidong Xiao, and Lei Li designed the project and wrote the manuscript. Cheng Ma, Ding Liu, and He Zhu performed the experiment. Cheng Ma, Ding Liu, and Xie-Feng Wan interpreted data. Dong Li, Xiao-Qian Xu, Carol H. Miao, and Barbara A. Konkle revised the manuscript. Philip Onigman provided the OpeRATOR enzyme and instructions.

CONFLICT OF INTEREST

The authors declare no conflict of interest.

SUPPORTING INFORMATION

Additional supporting information may be found online in the Supporting Information section.

¹³Bloodworks Northwest, Seattle, WA, USA

¹⁴Genovis Inc, Cambridge, MA, USA

Abstract

Background/Objective: Coagulation factor V (FV), a multidomain glycoprotein, is an essential cofactor in the blood clotting cascade. FV deficiency is a rare bleeding disorder that results in poor clotting after an injury or surgery. The only treatment for the disease is infusions of fresh frozen plasma and blood platelets. Glycosylation affects the biological activity, pharmacokinetics, immunogenicity, and in vivo clearance rate of proteins in the plasma. The glycan profile of FV, as well as how it affects the activity, stability, and immunogenicity, remains unknown.

Methods: In this study, we comprehensively mapped the glycosylation patterns of human plasma-derived FV by combining multienzyme digestion, hydrophilic interaction chromatography enrichment of glycopeptides, and alternated fragmentation mass spectrometry analysis.

Results/Conclusion: A total of 57 unique *N*-glycopeptides and 51 *O*-glycopeptides were identified, which were categorized into 40 *N*-glycan and 17 *O*-glycan compositions. Such glycosylation details are fundamental for future functional studies and therapeutics development. In addition, the established methodology can be readily applied to analyze glycosylation patterns of proteins with more than 2000 amino acids.

Keywords

coagulation factor V; glycosylation; HILIC; mass spectrometer

1 | INTRODUCTION

Human coagulation factor V (FV), also known as proaccelerin, is an essential glycoprotein involved in the clotting cascade. FV is expressed primarily in the liver. The 2224 amino acids (AAs) protein (including a 28 AAs signaling peptide) consists of six domains in the following sequence, A1, A2, B, A3, C1, and C2, similar to that of factor VIII (FVIII). FV and FVIII share approximately 40% AA sequence homology within A and C domains.^{1,2} Upon proteolytic activation by either thrombin or FXa, the B domain, which is unnecessary for the cofactor activity, is cleaved from FV. FVa complexed with FXa is involved in the process of converting prothrombin into thrombin, a vital step in the blood clotting process. Clinically, the rare bleeding disorder of FV deficiency is manifested as a prolonged blood clotting phenotype after an injury or surgery. Currently, fresh frozen plasma is used as the standard therapeutic option.³ However, the development of inhibitors to FV has been detected in certain FV-deficient patients after receiving fresh frozen plasma.^{4,5} FV concentrate, which is difficult to purify from plasma, was tested as an alternative but not widely used.⁶ Additionally, FV deficiency combined with FVIII deficiency results in a more severe hemophiliac phenotype.⁷

Glycosylation has been reported to play critical roles in protein folding,^{8,9} stability,^{10,11} macromolecular interactions, and activity.¹² Although the AA sequence within the B domain of FV apparently diverges between human and bovine genes, large numbers of glycosylation

sites are conserved, suggesting that glycosylation may provide a regulatory role for both the expression and activation of FV.¹³ On the other hand, glycosylation affects the function of FVa and is important for the interaction between FVa and other factors involved in the clotting cascade. For example, two isoforms of plasma FV that differ in glycosylation at Asn2209 in the C2 domain, FV1 (~33%) is *N*-glycosylated at this site, whereas FV2 (~67%) is not, showed different functionality.^{14,15} The activated FVa2 has a higher affinity for phospholipids than FVa1, thus has higher coagulant cofactor potency. It was shown that the *N*-glycosylation interfered with the formation of the FVa-FXa complex.¹⁵ In addition, total removal of *N*-glycans and terminal sialic acid on FVa by treatment with glycosidases resulted in increased activated protein C sensitivity, suggesting that glycosylation plays a role in activated protein C-catalyzed cleavage and inactivation of FV.¹⁶ Furthermore, a FV missense mutation Ile359Thr, which creates an additional *N*-glycosylation at Asn 357, could significantly reduce the cleavage at Arg306, thus affecting anticoagulation.¹⁷ Similarly, FVa mutants that contain unnatural *N*-glycosylation on position 495, 539, 680, or 1710 displayed attenuated FXa binding, which could be restored by inhibiting the expression of *N*-glycans, again implying the roles carbohydrates might play in FVa-FXa binding.¹⁸ Unlike Asn2209, these positions are located on A2 and A3 domains of FV. It is unknown whether these domains contain glycosylation and whether they play any functional roles. Nevertheless, comprehensive knowledge of the glycosylation of FV could provide fundamentals for understanding the roles and mechanisms of FV interactions in the coagulation cascade, in parallel to recently reported results on glycan profiling of FVIII.^{19–22} Additionally, such information and the method used to profile FV glycosylation could be of great importance in the development of FV-based pharmaceuticals because altered glycosylation was reported to affect the immunogenicity of glycoprotein drugs. For instance, non-human glycan structures (eg, alpha-gal, *N*-glycolylneuraminic acid) found in recombinant FVIII proteins were reported to increase their intrinsic immunogenicity.^{23,24} To date, a systemic analysis of FV glycosylation is still lacking.

In this work, we developed and applied an integrated approach for systematic glycan analysis of plasma-derived FV (pdFV). Glu-C and Trypsin were used for peptide digestion, and glycopeptide enrichment was performed by zwitterionic hydrophilic interaction chromatography (ZIC-HILIC). Alternated higher energy collisional dissociation (HCD) and electron-transfer dissociation (ETD) fragmentation were used to integrate *N*- and *O*-glycopeptide sequencing in one mass spectrometry (MS) analysis.²⁵ ¹⁸O-labeling of *N*-glycosylation sites and site-specific extraction of *O*-linked glycopeptide (EXoO) was also applied to localize exact *N*- and *O*-glycosylation sites.^{26,27} As a result, 108 unique glycopeptides comprising 12 *N*-glycosylation sites and 26 *O*-glycosylation sites were identified with the simultaneous determination of peptide sequences and glycoform compositions.

2 | MATERIALS AND METHODS

2.1 | Materials

Human pdFV was purchased from Haematologic Technologies. Trypsin (sequencing grade modified) and endoproteinase Glu-C (Glu-C) were supplied by Promega. PNGase F was

obtained from New England Biolabs. Sodium cyanoborohydride (NaCNBH₃), formic acid, ammonium hydrogen carbonate (NH₄HCO₃), and high-performance liquid chromatography grade acetonitrile (ACN) were purchased from Sigma-Aldrich. Dithiothreitol and iodoacetamide were obtained from Thermo Fisher. The 10-kDa Microcon centrifugal filter devices were purchased from Millipore. ZIC-HILIC material was bought from SeQuant; the 3M Empore C8 disk was purchased from 3M Bioanalytical Technologies; 10 µL extended pipet tips were from Axygen. The OpeRATOR/SialEXO kit was from Genovis, Inc. All chemicals used in the preparation of buffers and solutions were of analytical grade or better.

2.2 | Sample preparation and enzymatic digestion

Excipients in the pdFV sample were removed by passing through a 10-kDa Microcon centrifugal filter device. The buffer was changed to 50 mmol/L NH₄HCO₃ (pH 7.8), and the protein was concentrated to about 1 µg/µL. Filter-aided sample preparation was used to prepare MS analysis samples.²⁸ Briefly, this solution was incubated at 95°C for 10 minutes, and then centrifuged at 16,000g for 10 minutes. The resulting supernatant was mixed with 200 µL of 8 mol/L urea in 100 mmol/L Tris-HCl buffer, pH 8.5 (UA solution). The mixed sample was loaded into a 30 kDa Microcon filtration device and centrifuged at 14,000g until the remaining volume was less than 20 µL. The concentrate was then diluted in the filter device with 200 µL UA solution and centrifuged twice. Subsequently, the concentrate was mixed with 100 µL of 50 mmol/L iodoacetamide in the UA solution, incubated in darkness at room temperature for 30 minutes, and then centrifuged for 20 minutes. The concentrate was subsequently diluted with 200 µL of UA solution and concentrated again. The last step was repeated twice. The sample was then diluted with 100 µL 40 mmol/L NH₄HCO₃ and concentrated twice. After concentrating, 8 µg trypsin or 8 µg Glu-C in 100 µL 40 mmol/L NH₄HCO₃ (pH 7.8) or 100 µL 50 mmol/L NaH₂PO₄ (pH 7.5) was added for overnight digestion at 37°C. The resulting peptides were collected by centrifuging the filter units with 50 µL NH₄HCO₃ (pH 7.8) for 20 minutes. This step was repeated three times. The final concentration of peptides was determined by ultraviolet spectrometry (Nanodrop, Thermo) using an extinction coefficient of 1.1 for 0.1% (g/L) solution at 280 nm.

2.3 | Glycopeptides enrichment

Homemade HILIC SPE micro-tips were used for intact glycopeptide enrichment. A small piece of C8 membrane was taken from a 3M Empore C8 disk and pushed into the end of a 10 µL extended pipet tip using a blunt needle, and 2 mg ZIC-HILIC material was then packed as previously described.²⁹ The HILIC SPE micro-tip was washed with 100 µL of binding buffer (80% ACN/5% FA) twice. For sample loading, 100 µL of binding buffer was added to the dried sample and loaded onto the micro-tip three times to allow the binding of glycopeptides. The micro-tip was then washed with the binding buffer to remove non-glycopeptides, and glycopeptides were eluted with 100 µL of elution buffer (0.5% FA) twice. The flow-through was vacuum-dried and stored at -20°C until use. Glycopeptides (100 µg) enriched from proteolytic digested peptides were directly injected to MS for intact glycopeptide analysis.

2.4 | *N*-glycosite analysis

HILIC-enriched glycopeptides (100 µg) were dissolved with 50 µL of 50 mmol/L NH₄HCO₃ in H₂¹⁸O. PNGase F was then added, and the solution was incubated at 37°C for 12 hours to remove *N*-glycans. Deglycosylated peptides were desalted using Ziptip C18 (ZTC18S096, Merck Millipore Ltd), vacuum-dried, and preserved at –20°C for MS analysis.

2.5 | *O*-glycosite analysis

Approximately 200 µg of digested peptides were dissolved in 50 mmol/L NaH₂PO₄ (pH 7.5). The EXoO approach was used to identify *O*-glycosylation sites as previously reported.²⁷ Briefly, 200 µL Aminolink resin (Pierce) was incubated with the peptides in 50 mmol/L NaCNBH₃ and 50 mmol/L NaH₂PO₄ (pH 7.5) at room temperature overnight. The resin was then washed in a spin column and blocked by 50 mmol/L NaCNBH₃ and 1 mol/L Tris-HCl (pH 7.4) at room temperature for 30 minutes. After washing three times, the *O*-glycopeptides were released by OpeRATOR and SialEXO (1 unit/1 µg peptides each enzyme) in 20 mmol/L Tris-HCl (pH 6.8) at 37°C for 15 hours. The released *O*-glycopeptides were collected, desalted by a C18 SPE cartridge (Thermo Scientific), and dried for MS analysis.

2.6 | Liquid chromatography-tandem MS analysis of intact glycopeptides

Experiments were performed on an LTQ-Orbitrap Elite mass spectrometer equipped with EASY-spray source and nano-LC UltiMate 3000 high-performance liquid chromatography system (Thermo Fisher). An EASY-Spray PepMap C18 Column (length, 15 cm; particle size, 3 µm; pore size, 100 Å; Thermo Fisher) was used for separation. The separation was achieved with a linear gradient from 3% to 40% solvent B for 30 minutes at a flow rate of 300 nL/min (mobile phase A, 2% ACN, 98% H₂O, 0.1% FA; mobile phase B, 80% ACN, 20% H₂O, 0.1% FA). The LTQ-Orbitrap Elite was operated in data-dependent mode, and 10 most intense ions in MS¹ were subjected to collision-induced dissociation in the ion trap analyzer for deglycosylated peptide analysis, or alternated HCD and ETD fragmentation for intact glycopeptide analysis. The Orbitrap MS acquired a full-scan survey (mass-to-charge [*m/z*] range from 375 to 1500; automatic gain control target, 10⁶ ions; resolution at *m/z* 400, 60 000; maximum ion accumulation time, 50 ms). For collision-induced dissociation-MS, the default charge state was 3, the isolation width was *m/z* 3.0, normalized collision energy was 35%, activation Q was 0.25, and activation time was 5.0 ms. For alternated HCD and ETD-MS, the Orbitrap analyzer acquired HCD fragment ion spectra with a resolution of 15 000 at *m/z* 400 (automatic gain control target, 10 000 ions; maximum ion accumulation time, 200 ms). The LTQ analyzer acquired ETD fragment ion (automatic gain control target, 5000 ions; maximum ion accumulation time, 100 ms). In this acquired method, the five most intense ions were fragmented by HCD and ETD. The tandem MS scan model was set as the centroid. Other conditions used were S-lens RF level of ~60%, ion selection threshold of 50 000 counts for HCD.

2.7 | Data analysis

Data collected by the *N*-glycosite mapping experiment was processed with Proteome Discoverer 1.4 (Thermo Fisher Scientific). Peptide fragments were matched against the FV

protein sequence (UniProtKB entry P12259 or FA5_HUMAN), where iodoacetamide on Cys was used as static modification, oxidation of Met, and ^{18}O labeling of Asn ($m = 2.9848$) were used as a dynamic modification. The mass tolerance was set at 10 ppm for precursor ions and 0.5 Da for product ions. Trypsin and Glu-C were chosen for the enzyme, and two missed cleavages were allowed. A false discovery rate of 1% was estimated and applied at the peptide level. For intact *N*- and *O*-glycopeptide analysis, all spectra generated from glycopeptides were selected and combined into an mgf file with an in-house software based on the presence of HexNAc fragment ions of m/z 126.0549, 138.0549, 144.0655, 168.0760, and 204.0866 from HCD spectra. Theoretical masses of all possible peptides were calculated by a computer script and manually validated by PeptideMass (http://web.expasy.org/peptide_mass).³⁰ The online software GlycoMod (<http://web.expasy.org/glycomod/>) was used for intact *N*- and *O*-glycopeptide data interpretation. Alternated HCD and ETD fragmentation strategies were selected to analyze intact glycopeptide. To obtain precise glycopeptide sequences, we developed a data analysis strategy for intact glycopeptide sequencing. First, spectra of potential *N*- and *O*-glycopeptides were selected according to diagnostic ions from a series of HexNAc fragments. Second, all selected spectra were analyzed with GlycoMod and further verified manually according to Y1 ions ([peptide + GlcNAc]ⁿ⁺, $n = 1, 2, 3 \dots n$) and Y0 ions ([peptide]ⁿ⁺, $n = 1, 2, 3 \dots n$) from HCD-tandem MS spectra. Finally, HCD-associated ETD data were used for backbone sequencing. The workflow of MS data analysis is shown in Scheme S1.

3 | RESULTS

3.1 | N-glycosite microheterogeneity

By combining multiple enzymatic digestions, HILIC enrichment of glycopeptides, and alternated HCD and ETD fragmentations, 40 site-specific *N*-glycoforms (20 are core-fucosylated) and 12 *N*-glycosites were identified from pdFV with the simultaneous determination of peptide sequences and glycoform compositions (Table 1). Most *N*-glycosites on asparagine (Asn) residues within consensus sequences (Asn-x-Thr/Ser/Cys) were observed with glycan microheterogeneity, and 8 *N*-glycosites are identified with three or more glycoforms. Tandem MS annotations of *N*-glycopeptides were illustrated in Figures S1–S5. A total of 57 unique *N*-glycopeptides were identified. Among identified *N*-glycosites, our results showed that Asn382 is most heterogeneous, containing 17 glycoforms dominated by core-fucosylated ones. This site locates within the A2 domain of the heavy chain of FV. Ten glycoforms, including complex and high-mannose types, were identified at Asn554. On domain B, 4 *N*-glycosites were identified with various glycoforms. Among these sites, Asn938 contains seven glycoforms and four are core-fucosylated. Asn1074 and Asn1221 are occupied by complex and hybrid type *N*-glycans. The high percentage of core-fucosylated *N*-glycan in all identified glycoforms showed that pdFV is heavily glycosylated with core fucose. The core-fucosylation ratio in determined glycoforms is similar to that of FVIII.²⁰ The well-known immunogenic sialic acid form, *N*-glycolylneuraminic acid (Neu5Gc), was not observed in pdFV.

3.2 | Total relative abundances of the 40 *N*-glycoforms

We determined the relative abundance of detected glycoforms at each *N*-glycosite. Ion chromatograms of identified peptides extracted by LFQuant were used to quantify different glycopeptides. The *m/z* and retention time of glycopeptide precursor ions identified previously were used to extract ion chromatograms and calculate the peak area of individual glycopeptide. Peak areas were then normalized, and the relative abundance of each *N*-glycan composition was obtained regarding each site as shown in pie charts in Figure 1. Among 17 *N*-glycoforms identified at Asn382, monosialylated and core-fucosylated bi-antennary glycan H5N4S1F1 (**22**), monosialylated hybrid type glycan H5N3S1 (**11**), and asialylated core-fucosylated mono-antennary glycan H4N3F1 (**4**) are highly abundant, with 40%, 16%, and 10%, respectively. The top three highly abundant *N*-glycoform at Asn554 are all complex type, including disialylated core-fucosylated biantennary glycan H5N4S2F1 (**24**, 15%), asialylated glycan H4N3F1 (**4**, 15%), and monosialylated bi-antennary glycan H4N4S1 (**19**, 13%). Figure 2 illustrates the general distribution of FV *N*-glycome based on the 40 *N*-glycoforms. Top 2 abundant *N*-glycans are all complex types. The most abundant structure is the monosialylated H5N4S1F1 (**22**, 31.2%), which was defined on 4 *N*-glycosites, Asn297, Asn382, Asn1221, and Asn1703. The second abundant glycoform is the disialylated H5N4S2F1 (**24**, 20.1%) distributed on Asn297 and Asn382.

3.3 | *O*-glycosite microheterogeneity

FV was reported as highly *O*-glycosylated, with 53 possible sites (lacking glycoform information) identified from human serum samples, enriched by lectin VVA and PNA, which specific for Tn- and T-antigens.³¹ All these *O*-glycosites are located in the B domain, and many sites lack the exact position information.³¹ We focused on identifying exact *O*-glycosites and glycoforms at each site. HCD-MS² and ETD-MS² were used to profile FV *O*-glycosylation, and Figure 3 illustrated the corresponding spectra of one example glycopeptide APSHQATT⁸⁰⁵AGSPLR from pdFV. Tandem MS annotations of *O*-glycopeptides are shown in Figures S6–S11. Additionally, a recently developed method EXoO²⁷ was used to identify and double confirm the *O*-glycosites. In this method, a unique enzyme, OpeRATOR, selectively digest *O*-glycopeptide before the Thr/Ser residue where *O*-glycan locates, release a unique *O*-glycopeptide with an N-terminal Thr or Ser, thus enabling the identification of exact locations of *O*-glycosylation. The combination of the two methods enabled identification of totally 17 *O*-glycoforms on 26 *O*-glycosites (Table S1). As shown in Figure 4, 18 identified *O*-glycosites are localized within the B domain, 10 of which were identified before.³¹ The B domain of FV contains dozens of unusual 9 AA tandem repeat region,³² the EXoO method was able to locate 4 *O*-glycopeptides in this region: T₁₂₁₁TLSPD, T₁₂₃₈TLSPD, T₁₂₄₇TLSLDLSQ, and T₁₂₈₃TLSLDFSQ. Interestingly, *O*-glycoforms identified by HCD/ETD fragmentation on 3 sites (T1211, T1238, and T1283) share two sialylated structures (**43**, **45**) attached to the Thr. We did not observe the other 43 possible *O*-glycosites identified before, which may be a result of different enrichment approaches. The previous report used lectin enrichment that is more suitable for peptides with simple glycans such as Tn and T-antigens,³¹ whereas HILIC enrichment based on hydrophilic interaction with hydroxyl groups is more suitable for peptides with complex glycoforms. On the other hand, our method enabled the first identification of 1 *O*-glycosite

on the A1 domain (Ser310), 3 *O*-glycosites on the A3 domain (Ser1594, Ser1781, and Ser1868), 3 *O*-glycosites on the C1 domain (Ser1926, Thr1990/Thr1991, and Thr2053), and another *O*-glycosite on the C2 domain (Ser2090), most of which are occupied by complex *O*-glycans (Figure 4).

Among identified *O*-glycosites, Thr805 was most diversified, with seven glycoforms identified (Figure 4 and Table S1). Ser985 and Thr986 were the second most diversified *O*-glycosite with 6 glycoforms each. On FV, the core 1 (**42-45**) and core 2 (**46, 47, 49, 51-55**) structures were the major *O*-glycoforms, whereas some core 4 *O*-glycoforms were also identified (**56, 57**). The predominant *O*-glycoforms were sialyl-T antigen (**43**), disialyl-T antigen (**45**), and T antigen (**42**). Worth noting is that the *O*-glycans of pdFV is heavily sialylated. As shown in Table S1, Neu5Ac residues were observed on 13 of the total 17 identified *O*-glycoforms.

4 | DISCUSSION

The site-specific relative abundance of glycopeptides is becoming increasingly important in protein medicine, especially for pharmaceutical quality control. Although accurate and absolute quantitation is not possible in the absence of glycopeptide standards, relative abundances of various glycoforms at each *N*-glycosite were obtained in this study (Figure 2). Among the 57 site-specific *N*-glycoforms, the two highest abundant *N*-glycoforms are both biantennary complex structures. Unlike biantennary glycoforms, most multiantennary *N*-glycans are in relatively low abundance. The most abundant tri-(H6N5S1F1, **32**, 11.5%) and tetra-antennary (H7N6S1F1, **35**, 12.0%) *N*-glycan are both monosialylated and attached on Asn938. A monosialylated hybrid *N*-glycan H5N3S1 is distributed among two glycosites, Asn384 and Asn1221, with a total abundance of 21.3%. We observed that FV is highly fucosylated and sialylated, with around 84.2% of detected *N*-glycans decorated with core fucose (54.5%), Neu5Ac (50.9%), or both (22.8%), whereas non-core-fucosylated and nonsialylated glycoforms only account for about 15.8%. Such a high degree of sialylation is clearly important because activation of deglycosylated factor V was impaired, whereas removal of sialic acid resulted in a 1.5- to 2-fold increase in clotting activity.³³ The von Willebrand factor (VWF) was also known to be a highly sialylated hemostasis protein, which can bind to asialoglycoprotein receptor in the liver. Sialidase from infectious pathogens such as *Streptococcus pneumoniae* could decrease VWF sialylation, thus increasing its clearance.³⁴ Core-fucosylation is closely related to many diseases, and it has been reported to regulate protein function. For example, depletion of core fucose on Asn-297 of IgG1 significantly increases antibody-dependent cellular cytotoxicity activity,³⁵ and deletion of core fucose on α 3 β 1 Integrin reduces cell migration and attachment to the extracellular matrix.³⁶ Given the high degree of core-fucosylation on FV, it may also play a functional role in clotting, which needs further investigation.

Nicolaes and coworkers reported that glycans at Asn2209 could impair the interaction between FVa and the phospholipid membrane.¹⁴ Although glycosylation on Asn2209 is reported to affect FVa function, glycoform information on this site is lacking. Our results revealed that Asn2209 is mainly occupied by sialylated tetra-antennary *N*-glycans. We also identified another 11 *N*-glycosite on FV, one on the A1 domain, three on the A2 domain,

five on the B domain, one on the A3 domain, and another on the C1 domain. The heterogeneity of glycoforms on glycoproteins affects protein stability, activity, immunogenicity.^{37,38} In FV, Asn382 on A2 domain has 17 different glycoforms, thereby present high microheterogeneity. Some *N*-glycosites such as Asn752, Asn1074 on the B domain has only one or two glycoforms, which shows high homogeneity. It is reported that the introduction of glycosylation on A2 and A3 domains of FV attenuated FXa binding,^{17,18} but the roles of its natural glycosylation on these domains remain unclear. Our results provide fundamentals for future studies regarding the roles of such *N*-glycosylation to the functions of FV. One potential glycosite of interest is Asn1703. Regardless of structural similarities between FV and FVIII, their *N*-glycosylation are not conserved except for Asn1703, which corresponds to Asn1810 in FVIII. Our result indicated that they are both occupied with complex type *N*-glycans. Asn1810 on FVIII is thought to be involved in the interaction with LRP and lipid, and consequently plays important roles in the clearance and clotting activity of FVIII,³⁹ whereas the role of Asn1703 on FV is unknown.

Although *O*-glycosylation is thought to be on the B domain exclusively,^{31,40,41} we were able to identify 8 *O*-glycosites on A1, A3, C1, and C2 domains. Identified *O*-glycoforms of FV are mainly core 1 *O*-GalNAc structure, and T (42), sialyl-T (43), and disialyl-T antigen (45) occupy most of the *O*-glycosites. Core 2 *O*-GalNAc structures were also identified on several *O*-glycosites, especially T805. Such mucin-type *O*-GalNAc glycosylation is well known for its biological functions in cancer and immune system, and altered expression of Tn (41), sTn (43), and T antigen (42) were usually highly expressed in many types of cancers including gastric, colon, breast, and lung cancer.⁴² However, *O*-glycosylation in FV and other hemostasis proteins had rarely been studied, and the potential roles of *O*-glycans are yet to be revealed. Additionally, it is reported that heterogeneity of glycoforms on glycoproteins affects protein stability, activity, and immunogenicity.^{37,38} We identified two heterogeneous *O*-glycosites (T805 with 7 glycoforms, S985/T986 with six glycoforms), and several *N*-glycosites with high microheterogeneity (eg, Asn 382 [17 glycoforms], Asn554 [10 glycoforms]). These glycosites may be promising targets for further functional and mechanistic study, and our results provide a fundamental knowledge base.

5 | CONCLUSION

In summary, we comprehensively analyzed the glycosylation of pdFV by a strategy integrating multienzyme digestion, ZIC-HILIC enrichment, and alternated HCD and ETD. The implementation of different fragmentation strategies in one MS run and the combination of fragmentation strategies enabled us to acquire more information on both carbohydrate moieties and intact glycopeptides. Finally, a total of 57 unique *N*-glycopeptides and 51 *O*-glycopeptides were identified, categorized into 12 *N*-glycosites with 40 *N*-glycoforms, and 26 *O*-glycosites with 17 *O*-glycoforms, respectively. This glycosylation information is fundamental for further functional studies and FV-related therapeutic development.

Supplementary Material

Refer to Web version on PubMed Central for supplementary material.

ACKNOWLEDGMENTS

This work is supported by National Heart, Lung, and Blood Institute (U54HL142019).

REFERENCES

1. Vehar GA, Keyt B, Eaton D, et al. Structure of human factor VIII. *Nature*. 1984;312:337–342. [PubMed: 6438527]
2. Kane WH, Ichinose A, Hagen FS, Davie EW. Cloning of cDNAs coding for the heavy chain region and connecting region of human factor V, a blood coagulation factor with four types of internal repeats. *Biochemistry*. 1987;26:6508–6514. [PubMed: 2827731]
3. Huang JN, Koerper MA. Factor V deficiency: a concise review. *Haemophilia*. 2008;14:1164–1169. [PubMed: 19141156]
4. Kalafatis M. Coagulation factor V: a plethora of anticoagulant molecules. *Curr Opin Hematol*. 2005;12:141–148. [PubMed: 15725905]
5. Lee WS, Chong LA, Begum S, Abdullah WA, Koh MT, Lim EJ. Factor V inhibitor in neonatal intracranial hemorrhage secondary to severe congenital factor V deficiency. *J Pediatr Hematol Oncol*. 2001;23:244–246. [PubMed: 11846304]
6. Bulato C, Novembrino C, Anzoletti MB, et al. “In vitro” correction of the severe factor V deficiency-related coagulopathy by a novel plasma-derived factor V concentrate. *Haemophilia*. 2018;24:648–656. [PubMed: 29578313]
7. Tracy PB, Eide LL, Bowie EJ, Mann KG. Radioimmunoassay of factor V in human plasma and platelets. *Blood*. 1982;60:59–63. [PubMed: 7082847]
8. Helenius A. How N-linked oligosaccharides affect glycoprotein folding in the endoplasmic reticulum. *Mol Biol Cell*. 1994;5:253–265. [PubMed: 8049518]
9. Mitra N, Sharon N, Surolia A. Role of N-linked glycan in the unfolding pathway of Erythrina coralloidendron lectin. *Biochemistry*. 2003;42:12208–12216. [PubMed: 14567682]
10. Narhi LO, Arakawa T, Aoki KH, et al. The effect of carbohydrate on the structure and stability of erythropoietin. *J Biol Chem*. 1991;266:23022–23026. [PubMed: 1744097]
11. Shental-Bechor D, Levy Y. Effect of glycosylation on protein folding: a close look at thermodynamic stabilization. *Proc Natl Acad Sci USA*. 2008;105:8256–8261. [PubMed: 18550810]
12. Sharon N, Lis H. Lectins as cell recognition molecules. *Science*. 1989;246:227–234. [PubMed: 2552581]
13. Pittman DD, Tomkinson KN, Kaufman RJ. Post-translational requirements for functional factor V and factor VIII secretion in mammalian cells. *J Biol Chem*. 1994;269:17329–17337. [PubMed: 8006042]
14. Nicolaes GA, Villoutreix BO, Dahlback B. Partial glycosylation of Asn2181 in human factor V as a cause of molecular and functional heterogeneity. Modulation of glycosylation efficiency by mutagenesis of the consensus sequence for N-linked glycosylation. *Biochemistry*. 1999;38:13584–13591. [PubMed: 10521265]
15. Rosing J, Bakker HM, Thomassen MC, Hemker HC, Tans G. Characterization of two forms of human factor Va with different cofactor activities. *J Biol Chem*. 1993;268:21130–21136. [PubMed: 8407949]
16. Silveira JR, Kalafatis M, Tracy PB. Carbohydrate moieties on the procofactor factor V, but not the derived cofactor factor Va, regulate its inactivation by activated protein C. *Biochemistry*. 2002;41:1672–1680. [PubMed: 11814362]
17. Steen M, Norstrom EA, Tholander AL, et al. Functional characterization of factor V-Ile359Thr: a novel mutation associated with thrombosis. *Blood*. 2004;103:3381–3387. [PubMed: 14695241]
18. Steen M, Villoutreix BO, Norström EA, Yamazaki T, Dahlbäck BJ. Defining the factor Xa-binding site on factor Va by site-directed glycosylation. *J Biol Chem*. 2002;277:50022–50029. [PubMed: 12384508]

19. Sodetz JM, Paulson JC, Pizzo SV, McKee PA. Carbohydrate on human factor VIII/von Willebrand factor. Impairment of function by removal of specific galactose residues. *J Biol Chem.* 1978;253:7202–7206. [PubMed: 100492]
20. Kannicht C, Ramstrom M, Kohla G, et al. Characterisation of the post-translational modifications of a novel, human cell line-derived recombinant human factor VIII. *Thromb Res.* 2013;131:78–88. [PubMed: 23058466]
21. Thim L, Vandahl B, Karlsson J, et al. Purification and characterization of a new recombinant factor VIII (N8). *Haemophilia.* 2010;16:349–359. [PubMed: 19906157]
22. Canis K, Anzengruber J, Garenaux E, et al. In-depth comparison of N-glycosylation of human plasma-derived factor VIII and different recombinant products: from structure to clinical implications. *J Thromb Haemost.* 2018;16:1592–1603.
23. Kannicht C, Ramström M, Kohla G, et al. Characterisation of the post-translational modifications of a novel, human cell line-derived recombinant human factor VIII. *Thromb Res.* 2013;131:78–88. [PubMed: 23058466]
24. Lai JD, Swystun LL, Cartier D, et al. N-linked glycosylation modulates the immunogenicity of recombinant human factor VIII in hemophilia A mice. *Haematologica.* 2018;103:1925–1936. [PubMed: 30002126]
25. Singh C, Zampronio CG, Creese AJ, Cooper HJ. Higher energy collision dissociation (HCD) product ion-triggered electron transfer dissociation (ETD) mass spectrometry for the analysis of N-linked glycoproteins. *J Proteome Res.* 2012;11:4517–4525. [PubMed: 22800195]
26. Küster B, Mann M. ¹⁸O-labeling of N-glycosylation sites to improve the identification of gel-separated glycoproteins using peptide mass mapping and database searching. *Anal Chem.* 1999;71:1431–1440. [PubMed: 10204042]
27. Yang W, Ao M, Hu Y, Li QK, Zhang H. Mapping the O-glycoproteome using site-specific extraction of O-linked glycopeptides (EXoO). *Mol Syst Biol.* 2018;14:e84862018.
28. Wi niewski JR, Zougman A, Nagaraj N, Mann M. Universal sample preparation method for proteome analysis. *Nat Methods.* 2009;6:359. [PubMed: 19377485]
29. Gashash EA, Aloor A, Li D, et al. An insight into glyco-microheterogeneity of plasma von Willebrand factor by mass spectrometry. *J Proteome Res.* 2017;16:3348–3362. [PubMed: 28696719]
30. Wilkins MR, Lindskog I, Gasteiger E, et al. Detailed peptide characterization using PEPTIDEMASS—a World-Wide-Web-accessible tool. *Electrophoresis.* 1997;18:403–408. [PubMed: 9150918]
31. King SL, Joshi HJ, Schjoldager KT, et al. Characterizing the O-glycosylation landscape of human plasma, platelets, and endothelial cells. *Blood Adv.* 2017;1:429–442. [PubMed: 29296958]
32. Zhu H, Toso R, Camire RM. Inhibitory sequences within the B-domain stabilize circulating factor V in an inactive state. *J Biol Chem.* 2007;282:15033–15039. [PubMed: 17387173]
33. Bruin T, Sturk A, Ten Cate JW, Cath M. The function of the human factor V carbohydrate moiety in blood coagulation. *Eur J Biochem.* 1987;170:305–310. [PubMed: 3121323]
34. Pipe SW, Montgomery RR, Pratt KP, Lenting PJ, Lillicrap D. Life in the shadow of a dominant partner: the FVIII-VWF association and its clinical implications for hemophilia A. *Blood.* 2016;128:2007–2016. [PubMed: 27587878]
35. Shields RL, Lai J, Keck R, et al. Lack of fucose on human IgG1 N-linked oligosaccharide improves binding to human FcγRIII and antibody-dependent cellular toxicity. *J Biol Chem.* 2002;277:26733–26740. [PubMed: 11986321]
36. Takahashi M, Kuroki Y, Ohtsubo K, Taniguchi N. Core fucose and bisecting GlcNAc, the direct modifiers of the N-glycan core: their functions and target proteins. *Carbohydr Res.* 2009;344:1387–1390. [PubMed: 19508951]
37. Kolarich D, Lepenies B, Seeberger PH. Glycomics, glycoproteomics and the immune system. *Curr Opin Chem Biol.* 2012;16:214–220. [PubMed: 22221852]
38. Takahashi M, Tsuda T, Ikeda Y, Honke K, Taniguchi N. Role of N-glycans in growth factor signaling. *Glycoconj J.* 2003;20:207–212.

39. Kosloski MP, Miclea RD, Balu-Iyer SV. Role of glycosylation in conformational stability, activity, macromolecular interaction and immunogenicity of recombinant human factor VIII. *AAPS J.* 2009;11:424–431. [PubMed: 19499345]
40. Kane WH, Majerus PW. Purification and characterization of human coagulation factor V. *J Biol Chem.* 1981;256:1002–1007. [PubMed: 7451453]
41. Fernandez JA, Hackeng TM, Kojima K, Griffin JH. The carbohydrate moiety of factor V modulates inactivation by activated protein C. *Blood.* 1997;89:4348–4354. [PubMed: 9192757]
42. Fu C, Zhao H, Wang Y, et al. Tumor-associated antigens: Tn antigen, sTn antigen, and T antigen. *HLA.* 2016;88:275–286. [PubMed: 27679419]

Essentials

- Glycosylation affects the structure and functions of proteins.
- Comprehensive *N*- and *O*-glycome profiling of human coagulation factor V was performed.
- A total of 57 *N*-glycopeptides with 12 glycosites and 40 different *N*-glycoforms were identified from FV.
- Totally 51 *O*-glycopeptides with 17 *O*-glycoforms on 26 sites were determined.

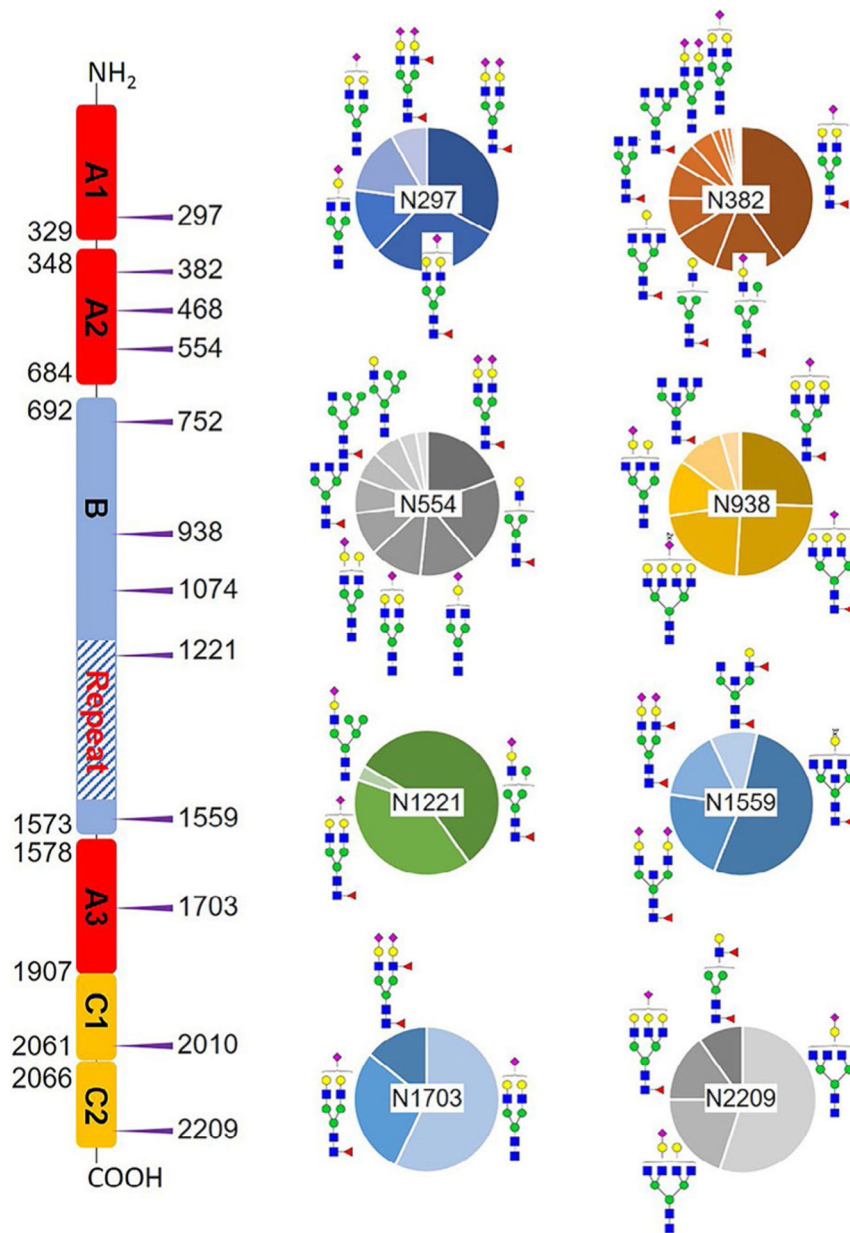


FIGURE 1. Microheterogeneity and relative abundance of *N*-glycoforms at 8 out of 12 FV *N*-glycosites. Only one glycoform was identified at Asn468, Asn752, and Asn2010. The assignment of domains is based on uniprot. Blue square, GlcNAc; green circle, Man; yellow circle, Gal; purple diamond, Neu5Ac; red triangle, Fuc.

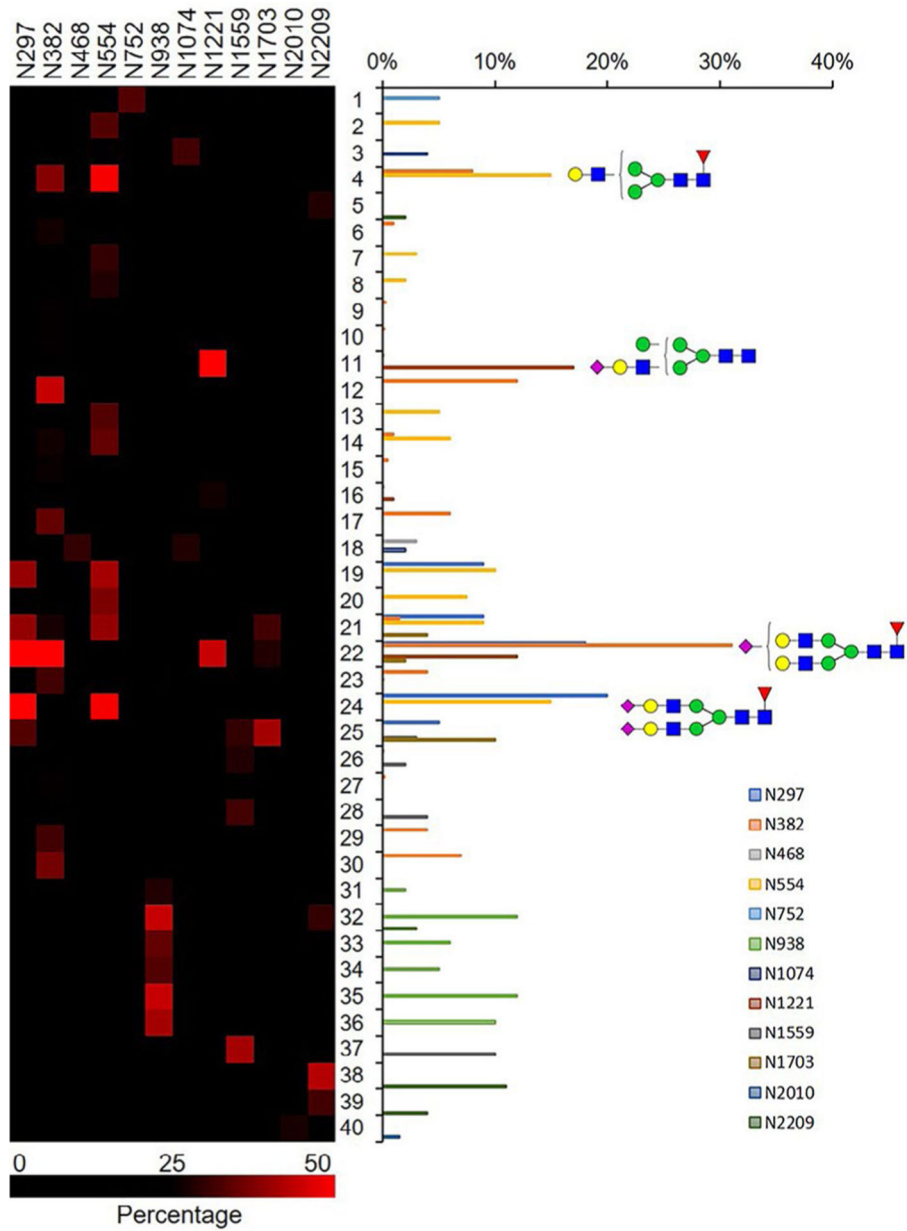


FIGURE 2. Distribution of *N*-glycan complexity. Total relative abundance of 40 *N*-glycans are represented in bar graphs. Blue square, GlcNAc; green circle, Man; yellow circle, Gal; purple diamond, Neu5Ac; red triangle, Fuc.

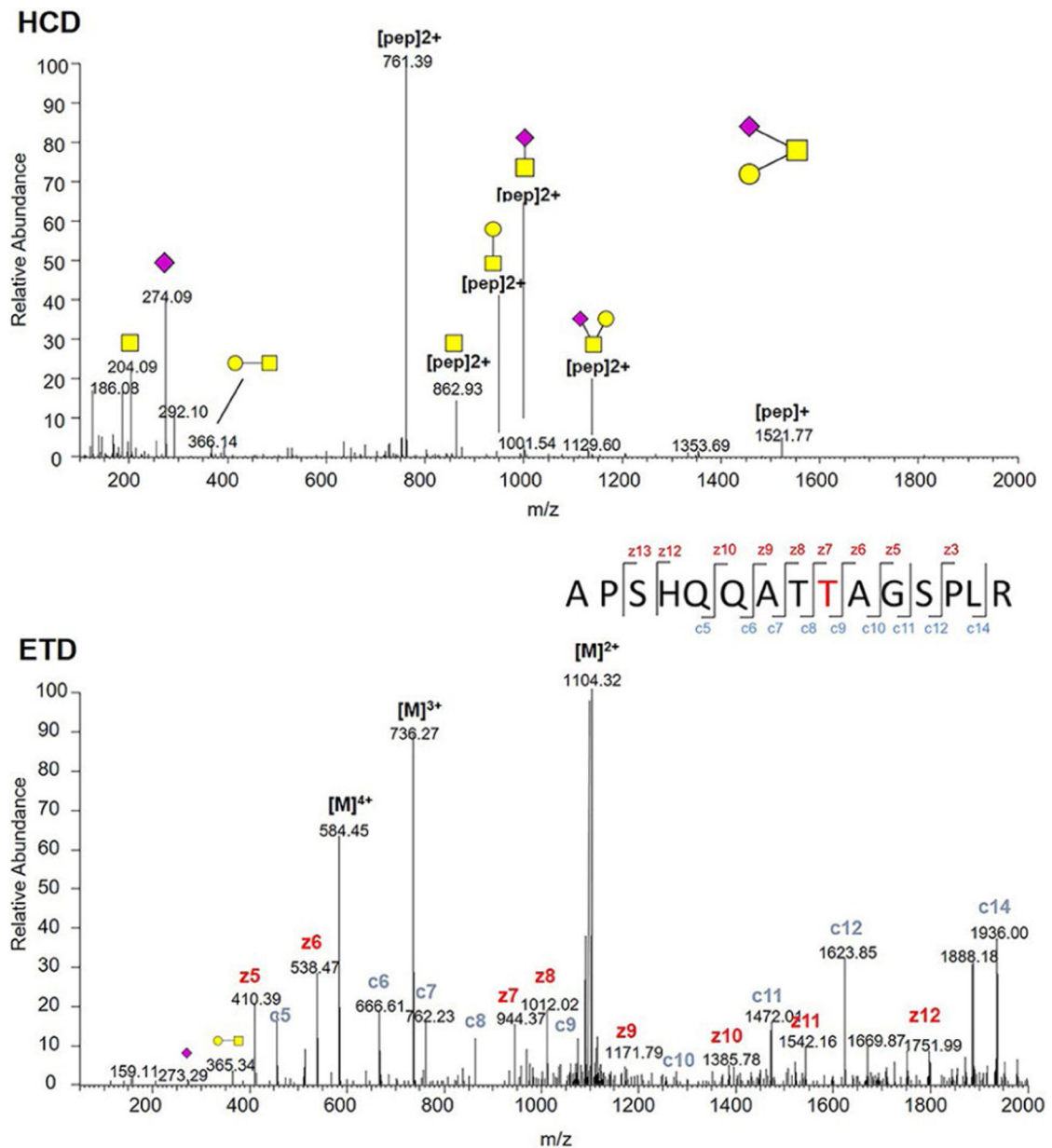


FIGURE 3. HCD-MS² (top) and ETD-MS² (bottom) spectra of (APSHQQATT⁸⁰⁵AGSPLR) glycopeptide derived from plasma-derived FV. Yellow square, *N*-acetylgalactosamine (GalNAc); yellow circle, Gal; purple diamond, Neu5Ac.

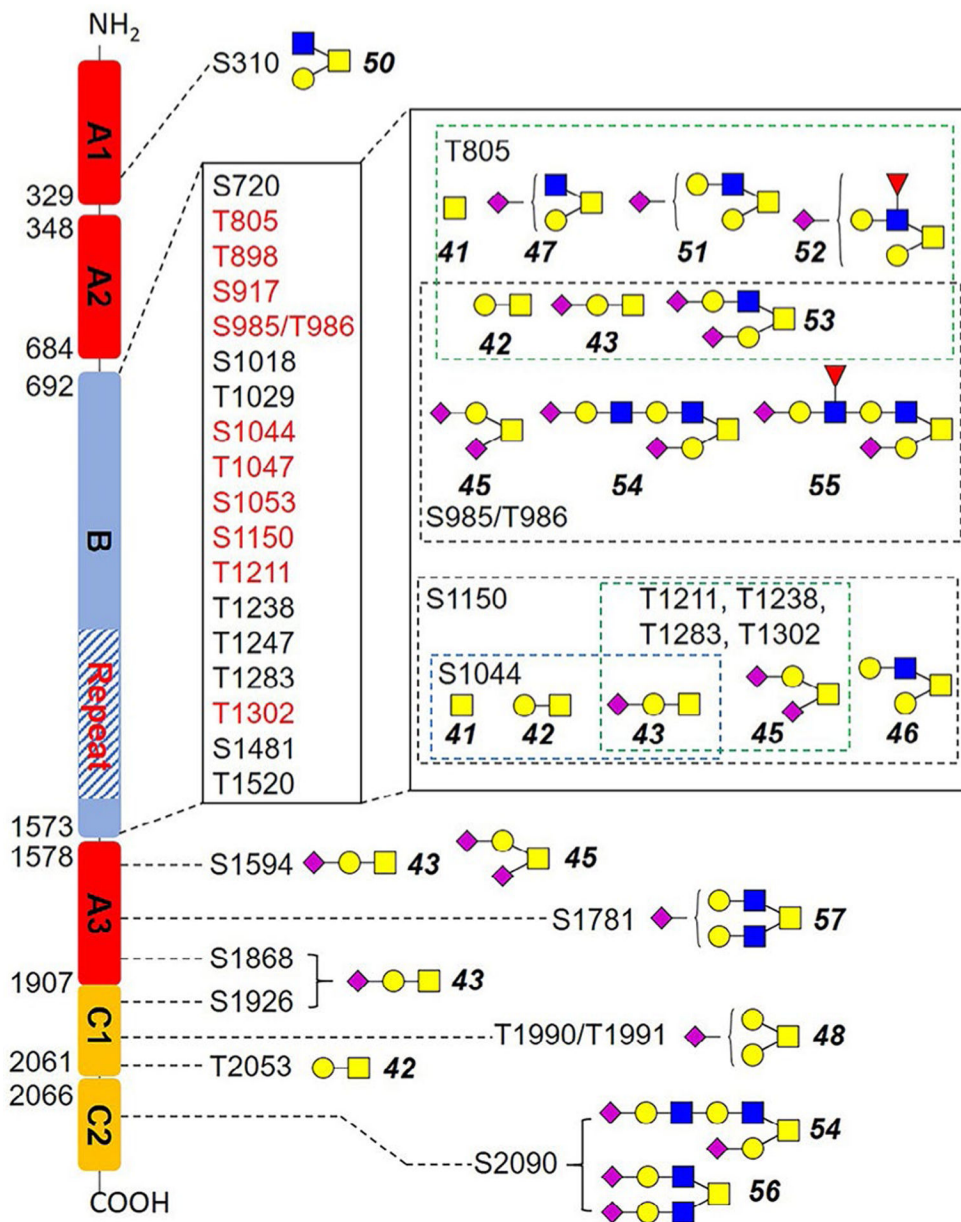
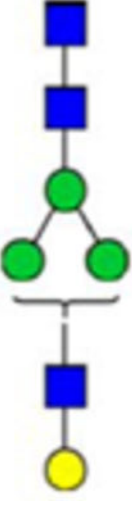
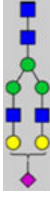
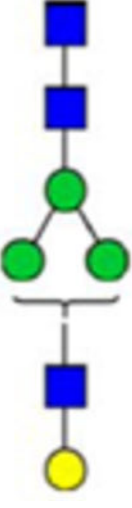
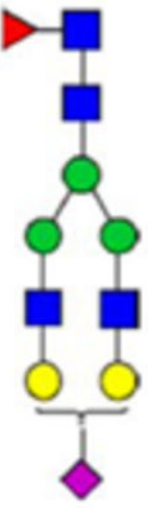
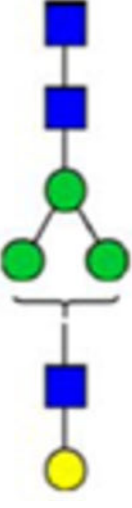
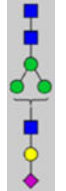
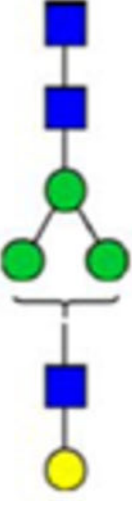
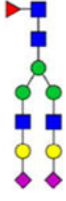
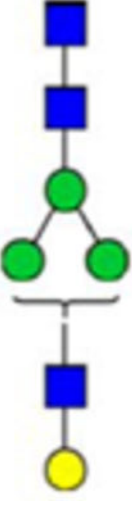
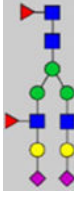
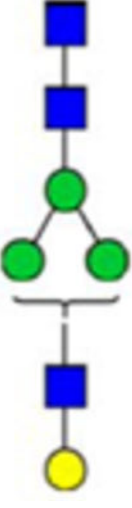
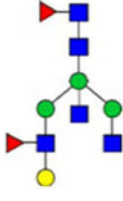
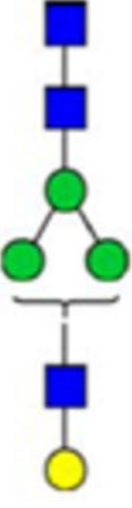
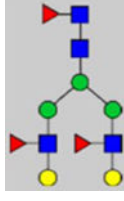
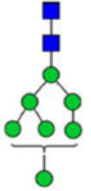
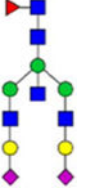
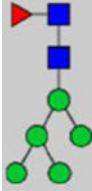
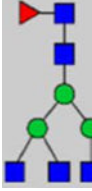
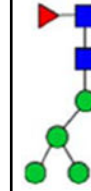
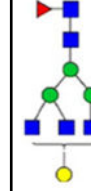
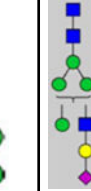
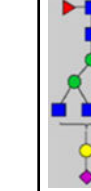
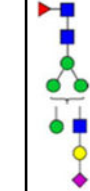
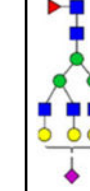
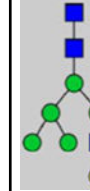
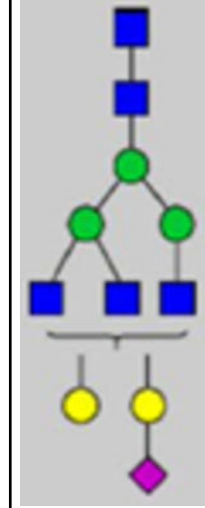
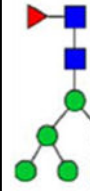
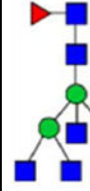

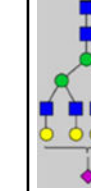


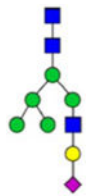
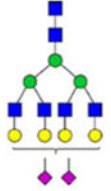
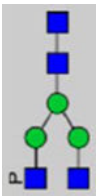
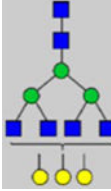
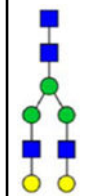
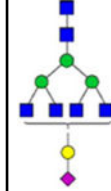
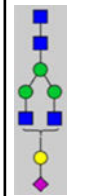
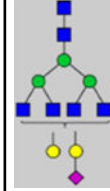
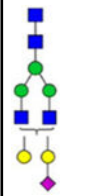
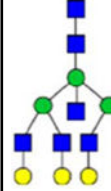
FIGURE 4. Identified *O*-glycosites and glycoforms on each site in this work. Red highlighted glycosites were also identified previously. Blue square, GlcNAc; yellow square, GalNAc; yellow circle, Gal; purple diamond, Neu5Ac; red triangle, Fuc.

TABLE 1

List of 40 identified N-glycoforms and 12 N-glycosites from FV

No.	Glycoform	Glycosite	No.	Glycoform	Glycosite
1		752	21		297, 382, 554, 1703
2		554	22		297, 382, 1221, 1703
3		1074	23		382, 938
4		382, 554	24		297, 554
5		2209	25		297, 1559, 1703
6		382	26		382, 1559
7		554	27		382

No.	Glycoform	Glycosite	No.	Glycoform	Glycosite
8		554	28		1559
9		382	29		382
10		382	30		382
11		382, 1221	31		938
12		382	32		938, 2209
13		554	33		938
14		382, 554	34		938
15		382	35		938

No.	Glycoform	Glycosite	No.	Glycoform	Glycosite
16		382, 1221	36		938
17		382	37		1559
18		468, 1074	38		2209
19		297, 554	39		2209
20		554	40		2010

Note: Blue square, N-acetylglucosamine (GlcNAc); green circle, Mannose (Man); yellow circle, Galactose (Gal); purple diamond, N-acetylneuraminic acid (Neu5Ac); red triangle, L-Fucose (Fuc).